

Photophysical Studies on the Mono- and Dichromophoric Hemicyanine Dyes II. Solvent Effects and Dynamic Fluorescence Spectra Study in Chloroform and in LB Films

Yanyi Huang, Tianrong Cheng, Fuyou Li, Chuping Luo, and Chun-Hui Huang*

State Key Laboratory of Rare Earth Materials Chemistry and Applications, College of Chemistry and Molecular Engineering, Peking University, Beijing 100871, China

Zhigang Cai, Xueran Zeng, and Jianying Zhou

State Key Laboratory of Ultrafast Laser Spectroscopy, Zhongshan University, Guangzhou 510275, China

Received: April 3, 2002; In Final Form: July 13, 2002

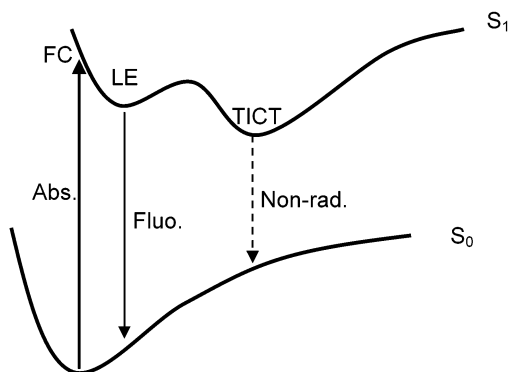
A series of hemicyanine dimers, (B3, B5, and B12) whose two chromophores are linked by different numbers of methylene groups, are synthesized. Negative solvatochromic behaviors are observed, and the fluorescence quantum yield is sensitive to the polarity of solvent. In chloroform, the fluorescence intensity is much more intensive than in other polar solvents, and the decay lifetime is much longer. This fluorescence sensitivity to solvent is due to the twisted intramolecular charge transfer (TICT) state formation, which can be blocked in weak polar solvent. The two chromophores in one dimer molecule are correlated and the TICT formation of dimer is relatively difficult compared with monomer. When the linkage is long enough, this correlation can be reduced. The dynamic fluorescence spectra of the chloroform solutions of these dyes support our assumption. The time-resolved fluorescence studies of their LB films provide a new perspective on the excited-state deactive process. The two-dimensional Förster energy transfer between the chromophores within monolayer is assumed to play an important role of their excited states in these LB samples. The difference of the proportions of energy transfer is supposed to be the responsible for the difference of their photoelectro conversion efficiencies.

1. Introduction

Aminostilbazolium (hemicyanine) is a common fluorescence probe for electrical membrane potential in biochemistry and biophysical area.^{1,2} It is also a very important fluorescence dye applied to lasers,³ molecular electronics,⁴ and nonlinear optical photo limiting devices.⁵ Actually, hemicyanine chromophore, which has the electron pushing (donor) group on one end and the electron withdrawing (acceptor) group on the other, has an extremely large first-order hyperpolarizability (β). It is one of the most efficient molecular based materials for the second harmonic generation (SHG).^{6–11} In recent years, we have reported the relationship between chromophore structures and SHG property, as well as the photoelectro conversion property of hemicyanine and its derivatives.^{12–15} Furthermore, as a fluorescence probe with large multiphoton absorption cross section, hemicyanine and related molecules have been applied to up-conversion emission material¹⁶ and the efficient up-converter for multiphoton fluorescence microscopy,¹⁷ which has great application potentiality.

The reaction scheme of excited state of stilbazolium has been proposed by Formherz et al.¹⁸ and then slightly modified by Bohn et al.^{19a} Here, we simplify the model as shown in Chart 1, in which only local excited (LE) and twisted intramolecular charge transfer (TICT) states are considered for the potential energy surface of excited state. This simplification is based on the photophysical properties of hemicyanine reported before.²⁰ Generally speaking, the trans-cis isomerization is not favorable in the excited state, whereas the TICT state formation dominates

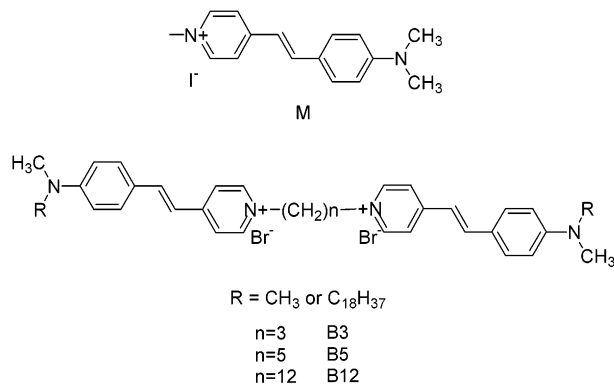
CHART 1: Schematic Illustration of the Potential Energy Surface of the Singlet Excited State S_1 and Ground State S_0 . FC: Franck–Condon State; LE: The Equilibrium Local Excited State; TICT: Twisted Intramolecular Charge Transfer State



the evolution of excited state of hemicyanine. Unlike the usual situation among most TICT species, this TICT state is not mainly formed by twisting around the dimethylamino group (C–N single bond), but by twisting around the aniline ring (C–C single bond). The torsion mode of twisting the aniline ring will be a barrierless process in polar solvents. Thus, Chart 1 can be seen as a simplified model to demonstrate the excited-state deactive processes of hemicyanine and related derivatives. The TICT state plays an important role in photophysical properties of hemicyanine. One of the common characteristic of the TICT state is the dual fluorescence of the donor–acceptor chromophores.^{21–24} However, the TICT state of hemicyanine is assumed to be nonradiative.²⁵ Recently, McHale et al. have

* To whom the correspondence should be addressed. E-mail: hch@chem.pku.edu.cn.

SCHEME 1: Chemical Structures of Hemicyanine Dyes. M: Monomer; B3, B5, and B12: Dimers with Difference Length of Linkages between the Chromophores



confirmed the TICT formation and its nonradiative feature by the method of ultrafast resonance Raman spectroscopy and theoretical computations.^{26–28}

With the development of molecular electronics and the increasing demand for molecular devices, more and more attention has been paid to supramolecular organizations such as aggregates²⁹ and molecular dimers,^{30–37} not just the individual or isolated molecule. Usually, the macroscopic properties, especially the photoactive properties such as absorption, emission, or nonlinear optical properties, strongly depend on the interaction between the different chromophores. The most common spectroscopic behavior of aggregate is the shift of the absorption peaks. According to the exciton coupling theory,³⁸ blue-shift is due to the formation of H-aggregate while red-shift the J-aggregate. The formation of aggregates can be tuned by external environments and the “intramolecular aggregate” can also be generated by joining two chromophores with proper linkage.^{35,37} Meanwhile, an interchromophore delocalization occurs in bichromophoric paracyclophanes when the orientations of those chromophores are appropriate.^{30,36}

In this paper, we present results of solvents effects of a series of hemicyanine dimers as well as their dynamic fluorescence spectra in certain solvents and in LB films. The difference of the three dimers (named as B3, B5, and B12, see Scheme 1) is the length of the linkage between the two hemicyanine chromophores because the linkage is an alkyl chain consisted of different numbers of methylene groups. Only in some really weak polar solvents such as tetrahydrofuran and ethyl acetate, can H-aggregate be clearly observed. The high fluorescence quantum yields of these dyes in weak polar solvent chloroform support the potential energy surface plotted in Chart 1. The difference among fluorescence decay lifetimes of the dimers and the monomer indicates that the chemical structure can affect the formation of TICT state. The different values of fluorescence lifetime of their LB films suggest that the two-dimensional energy transfer exists in their LB films and the reduction of energy transfer in B3 and B5 is the reason for their higher photoelectro conversion quantum yields.

2. Experimental Section

All the hemicyanine dyes (Scheme 1), monomer (M) and dimers (B3, B5 and B12) are synthesized by condensation reactions between a proper benzaldehyde and 4-methylpyridinium halide derivatives. The details of our method will be reported elsewhere and similar reactions have been published by Mishra et al.^{32,33} The structures and purities are identified by NMR, elements analysis and IR. All solvents are A. R. grade and purchased from Beijing Chemical Factory, China.

Absorption spectra at ultraviolet and visible regions are recorded by a UV-3100 UV–vis–NIR spectrophotometer (Shimadzu Co., Japan), with blank solvents as reference. Fluorescence spectra are measured by a F4500 fluorescence spectrophotometer (HITACHI Co. Japan), proper high-pass optical filters were used to remove the excitation light.

The transient luminescent spectra at room temperature are recorded by a synchroscan streak camera (temporal disperser C1587, tuning unit M1954, digital camera C4742–95, Hamamatsu Co., Japan). The exciting source is a CW mode locked Nd:YAG laser (Spectra-Physics, USA) with SHG (532 nm output, 82 MHz). The pulse width of laser is 80 ps. The data process and analysis are carried by HiPic software (Ver 5.1.0, Hamamatsu, Japan) and home-written programs.

The fluorescence dynamics of dyes at low temperature (77 K) are measured by similar setup as at room temperature. The exciting light is a Ti:sapphire laser (Spectra-Physics, Tsunami 3950-L2S, 1.5 ps FWHM) pumped by a Ar⁺ laser (Spectra-Physics, BeamLok 2060–10SA). A pulse-picker (Spectra-Physics Model 3980) reduces the repetition to 2 MHz. The second harmonic generator (GWU-23PS) is employed to generate the 410 nm laser, which irradiates the samples. The fluorescence signal is collected by a C4334–01 Streak Camera (Hamamatsu, Japan).

A Nima 622 Langmuir–Blodgett trough (Nima Ltd., Coventry, UK) is used for LB film fabrication. The subphase, ultrapure water (18 MΩ cm, pH 5.6), is made by an EASY pure water compact purifier (Barnstead, USA), and the temperature is controlled at 298 K throughout the experiments. The compressing speed of float Langmuir film is 50 cm² min⁻¹ and the dipping speed is 3 mm min⁻¹. The substrate is polished quartz slides and each experimental result is repeated by at least three individual samples.

3. Results and Discussion

3.1. Steady-State Spectra. It is well-known that hemicyanine has a strong absorption band around 500 nm, which comes from the charge-transfer transition. Extensive researches on hemicyanine and its derivatives in the past two decades show that hemicyanine chromophore has negative solvatochromic behavior (absorption peak position blue-shifts through the increase of the solvent polarity), indicating that the ground state has larger dipole moments than excited state (Franck–Condon region). Figure 1 shows the absorption (a) and fluorescence (b) spectra of monomer (M) in three different common solvents: propylene carbonate (PC), ethanol and chloroform. Generally speaking, the polarities of these solvents are in the following order: PC > ethanol > chloroform. The absorption spectra evidently show the negative solvatochromic behavior of M. Furthermore, solvation also strongly affects the fluorescence spectra (Figure 1(b)). The shapes of these spectra are similar in all solvents except tetrahydrofuran (THF) and ethyl acetate (EtAc), whose spectra are shown in Figure 2. The spectra of M in THF and in EtAc have evident absorption bands around 300 and 370 nm, which are very different from the absorption band around 500 nm. It is worth noting that these solvents, THF and EtAc, are both weak polar ones. The 370 nm absorption can be assigned as the transition between the ground state and excited state of the hemicyanine aggregates, whereas the 300 nm absorption is the S₀ → S₂ transition.^{19d}

An important feature of hemicyanine dye and its derivatives is that they can easily form aggregates in solvents and confined regions (such as monolayers). According to the results of absorption spectra of hemicyanine and the exciton theory, the

TABLE 1: Solvents Parameters and Steady State Spectroscopic Data of Dyes

solvent	parameters						absorption (cm ⁻¹)				fluorescence (cm ⁻¹)			
	ϵ	n	Δf	F	π^*	E_T^N	M	B3	B5	B12	M	B3	B5	B12
propylene carbonate (PC)	64.92	1.420	0.287	0.70	0.83	0.491	21141.6	20618.6	20920.5	21097.0	16666.7	16556.3	16583.7	16611.3
acetonitrile	35.94	1.342	0.305	0.71	0.75	0.460	21276.6	20491.8	20920.5	21141.6	16528.9	16420.4	16528.9	16611.3
dimethyl sulfoxide	46.45	1.478	0.263	0.66	1.00	0.444	21231.4	20618.6	20876.8	21008.4	16393.4	16393.4	16393.4	16474.5
ethanol	24.55	1.359	0.290	0.67	0.54	0.654	20833.3	20000.0	20325.2	20661.2	16835.0	16638.9	16722.4	16863.4
acetone	20.56	1.356	0.285	0.65	0.71	0.355	21097.0	20661.2	21008.4	21008.4	16611.3	16447.4	16556.3	16611.3
chloroform	4.81	1.443	0.149	0.29	0.58	0.259	20000.0	19960.1	20242.9	20366.6	17094.0	17667.8	17421.6	17241.4
ethyl acetate	6.02	1.370	0.201	0.40	0.55	0.228	21551.7				16806.7			
tetrahydrofuran	7.58	1.405	0.210	0.44	0.58	0.207	20703.9				16949.2			
2-propanol	19.92	1.375	0.277	0.63	0.48	0.546	20964.4	20040.1	20576.1	20491.8	16920.5	16835.0	16863.4	16949.2
pyridine	12.91	1.510	0.214	0.50	0.87	0.302	20242.9	20080.3	20408.2	20449.9	16528.9	16722.4	16778.5	16722.4
dimethylformamide	36.71	1.428	0.275	0.67	0.88	0.404	21231.4	20618.6	20920.5	21141.6	16778.5	16474.5	16474.5	16611.3
water	78.3	1.333	0.320	0.76	1.09	1.000	22321.4	21459.2	21881.8	21645.0	16750.4	16750.4	16750.4	16750.4
methanol	32.66	1.328	0.309	0.71	0.59	0.762	21008.4	20242.9	20661.2	20920.5	16778.5	16556.3	16666.7	16750.4

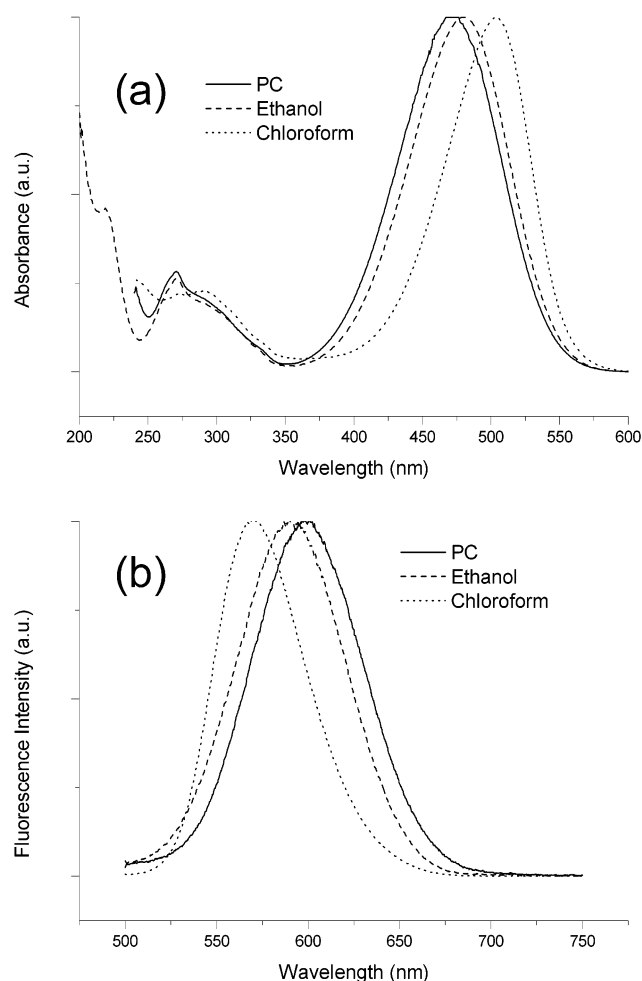


Figure 1. Steady-state spectra of M in three typical solvents: propylene carbonate (PC), ethanol and chloroform. (a) absorption spectra; (b) fluorescence spectra, excitation wavelength is 420 nm.

usually observed large blue-shifted absorption peak is originated from H-aggregates. It has been confirmed that the H-aggregate has an absorption peak around 350 nm and that the formation of H-aggregate strongly depends on experimental environments.^{19b,19c} Hence, the strong absorption around 370 nm in THF and EtAc is evidently a result of the formation of the H-aggregates in these solvents. It is very interesting to find the relationship between the formation of aggregate and the properties of the solvents. Obviously, among those solvents we have investigated in this work, THF and EtAc has the minor

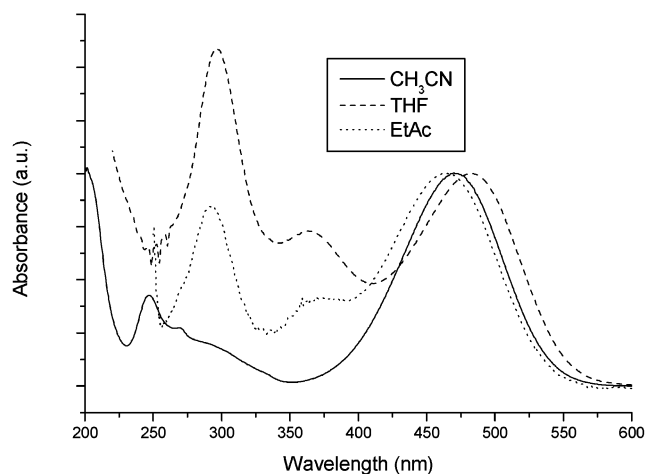


Figure 2. Absorption spectra of M in acetonitrile (CH₃CN), tetrahydrofuran (THF) and ethyl acetate (EtAc).

polarities (see Table 1 for those solvent parameters of these solvents). The possible reason for this phenomenon might be the high dipole moments of the hemicyanine chromophore: weaker polar solvents do not favor the high polar solute molecule. Thus, those high polar hemicyanine molecules are not well “dissolved” in weak polar solvents but prefer to disperse into aggregates. Our test shows that the solubility of M in such weak polar solvents is extremely small: smaller than 1×10^{-6} mol dm⁻³ at room temperature even under long-time ultrasonic treating. And those dimers (B3, B5, and B12) cannot dissolved in THF or EtAc at all.

However, there is an exception among the minor-polar-solvents. Although there is an absorption peak around 300 nm in the chloroform solution of M, the absorption is rather weak. Meanwhile, those chloroform solutions of dimers have no additional absorption peak around 300 nm, indicating chloroform is not a good solvent for aggregate formation. Furthermore, quite a few experimental results (see below) of hemicyanine photo-physical properties in chloroform show that chloroform is a very unique solvent for these molecules.

It is found in some dye molecules that the solution concentration can remarkably influence the formation of aggregate and consequently the absorption spectrum.²⁹ We have investigated the relationship between the absorption spectra and the concentration of the solution of M in methanol (Figure 3) and discover that nothing changes with the shape of the spectra and no new absorption peak appears when the concentration is increased. Experiments on dimers render the similar results

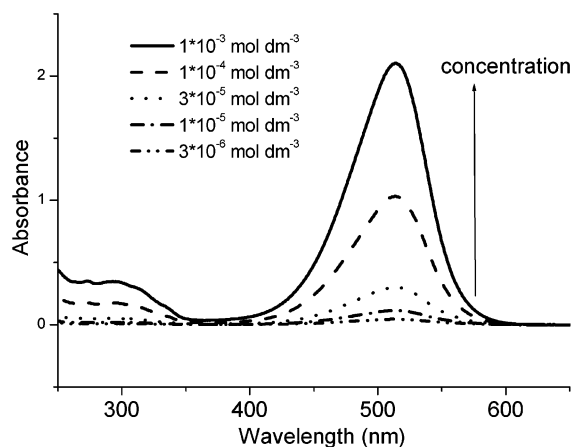


Figure 3. Absorption spectra of M in methanol with different concentrations (from $3 \times 10^{-6} \text{ mol dm}^{-3}$ to $1 \times 10^{-3} \text{ mol dm}^{-3}$, the thickness of the each solution sample is not a constant).

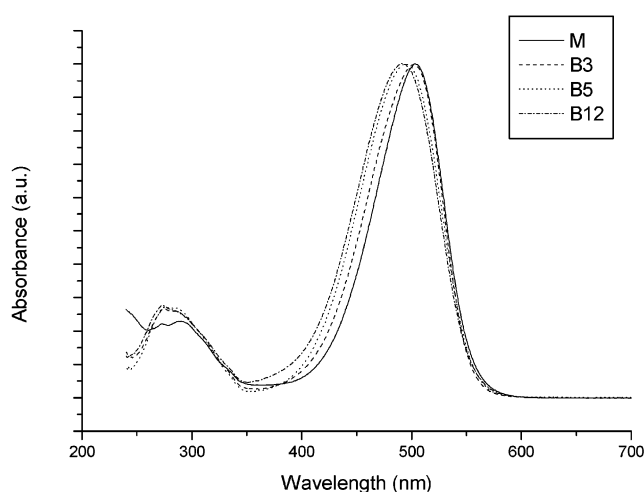


Figure 4. Absorption spectra of dyes in chloroform.

(spectra not shown here), which imply that the formation of aggregate is mainly controlled not by the intermolecular interaction between solute molecules/chromophores but by the interaction between the solute molecule and surrounding solvent molecules. And the similarity between the spectra of monomer and dimers also supports this hypothesis. It is an easy way to compare the difference between the absorption spectra of monomer and of dimers to determine the interaction between the two chromophores within one dimer molecule. But our results (Figure 4) clearly show that the dimerization brings no notable changes onto the transition from the ground state to the excited state of hemicyanine. If the interaction between the two chromophores in a dimer molecule is strong enough, there will be an "intramolecular aggregate". Although the molecular simulation of B5 has predicted a favorable folded conformation, in which the two chromophores of B5 are almost parallel and the distance between these two chromophores is quite close ($\sim 0.5 \text{ nm}$), there is no evidence for the existence of "intramolecular aggregates". Obviously, this is because of the strong static repulsion between the two partial positive charged pyridium moieties of two chromophores in a dimer molecule. If the dimer molecule can dissolve in a solvent, then the two chromophores trend to be separated to reduce the repulsive force; otherwise, they tend to form an aggregate structure to reach a stable state. Among all of the solvents studied here, hemicyanine has poor solubility in THF and EtAc; in chloroform, the solubility is better; and in major polar solvents, such as methanol, ethanol,

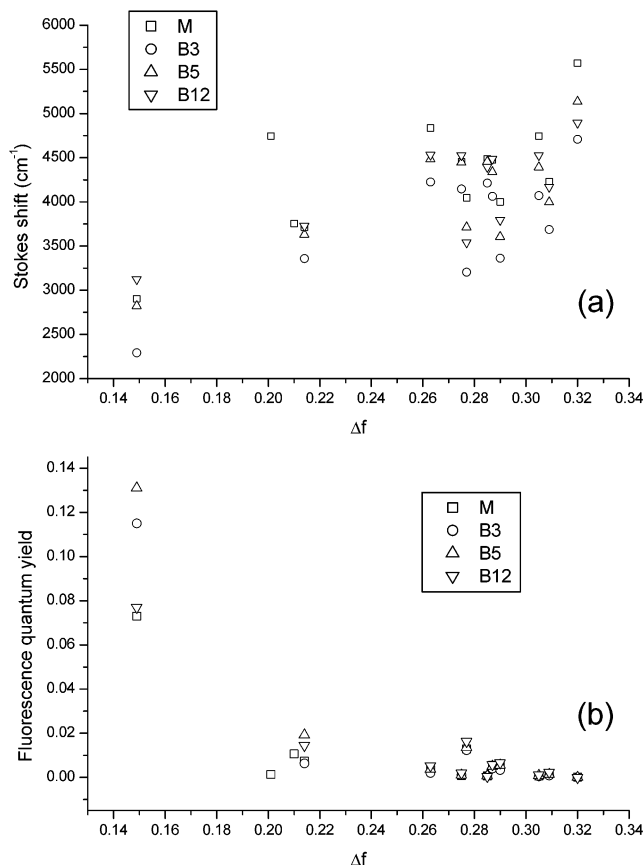


Figure 5. Relationship between the Stokes shift $\Delta\nu$ (a), the quantum yield (b) and the orientation polarizability Δf .

PC, and acetonitrile, the solubility is really good. Thus, we can clearly observe the aggregate formation in THF and EtAc but not in high polar solvents.

3.2. Solvation Effects: Solvent Parameters and Spectra.

It is observed that the Stokes shift changes remarkably with the change of solvents. Usually, the Stokes shift is a function of the orientational polarizability (Δf) and is given by the Lippert equation^{3,24,29,39-42}

$$\Delta\nu = \nu_{\text{abs}} - \nu_{\text{em}} = \frac{|\Delta\mu|^2}{2\pi\epsilon_0 h c a^3} \Delta f + \text{const} \quad (1)$$

where

$$\Delta f = \left(\frac{\epsilon - 1}{2\epsilon + 1} - \frac{n^2 - 1}{2n^2 + 1} \right) \quad (2)$$

where ϵ and n are dielectric constant and optical refractive index, respectively; h is Planck's constant, c is the speed of light, and a is the radius of the cavity in which the fluorophore resides. Figure 5 through 8 are the relationship between the photophysical properties and the solvent parameters. The details on these relationships will be discussed later. Figure 5a shows the Lippert relationship between the experimental results of the Stokes shift and the orientational polarizability of solvents. The first noteworthy feature is that three solvents stray away from the roughly linear relationship: methanol, ethanol, and propanol. This indicates that there might be specific interaction between the solute chromophore and these three solvents molecules because the Lippert equation is suitable only for nonspecific interaction. The basic theory underlying the Lippert equation estimates the solvation process, often named as Onsager's

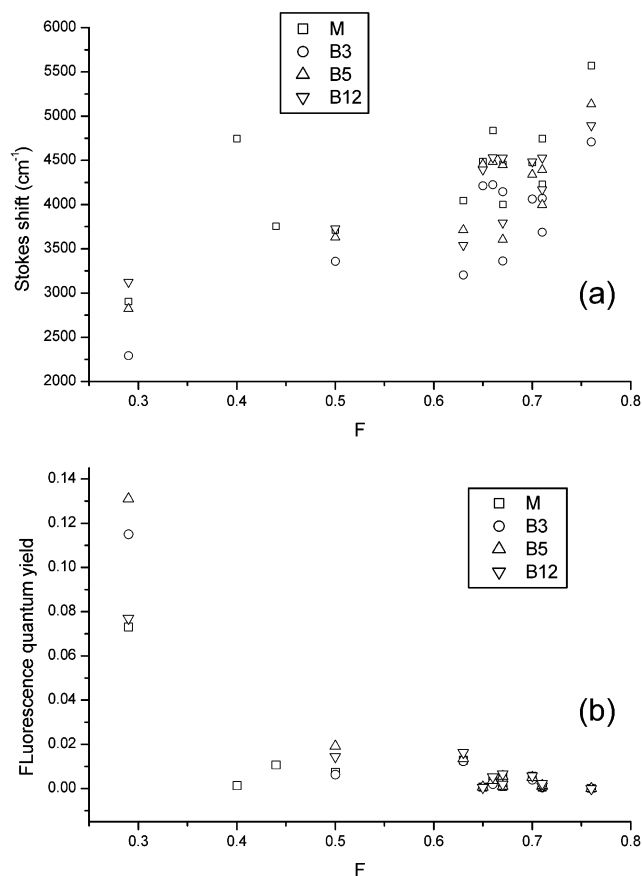


Figure 6. Relationship between the Stokes shift $\Delta\nu$ (a), the quantum yield (b) and the reaction field factor F .

reaction field model, by which the solute–solvent interaction is defined as a function of dielectric constant and optical refractive index of solvent. Another common parameter derivative from the same model is the reaction field factor F . Generally, the solvation energy can be expressed by^{23,43–45}

$$\Delta E_{\text{sol}} = \frac{2\mu^2}{r^3} \left(\frac{\epsilon - 1}{\epsilon + 2} - \frac{n^2 - 1}{n^2 + 2} \right) \quad (3)$$

Here, μ and r are dipole moment and diameter of solute molecule, respectively; the expression in the bracket is the reaction field factor

$$F = \left(\frac{\epsilon - 1}{\epsilon + 2} - \frac{n^2 - 1}{n^2 + 2} \right) \quad (4)$$

The relationship between the Stokes shift and the F factor is plotted as Figure 6(a). It is very similar to Figure 5a, and the three stray solvents in the Δf scale are also strays in the F scale.

Several parameters have been defined to describe the differences between the properties of solvents (see Table 1 and refs 29,43,46–49). π^* and E_T^N are often used to scale the polarizability of solvent. Figure 7(a) and 8(a) show the relationship between the Stokes shifts and polarizability of solvents, which is expressed as π^* and E_T^N , respectively. It is difficult to find a linear relationship between the Stokes shifts and E_T^N ; the change tendency can be divided into at least two parts by the point $E_T^N = 0.5$. The points in the region $E_T^N > 0.5$ is the results from methanol, ethanol, propanol and water solutions. These four points for each dye molecule have a roughly linear relationship but this linearity cannot be extrapolated to smaller E_T^N region. This indicates that the solvents in these two different

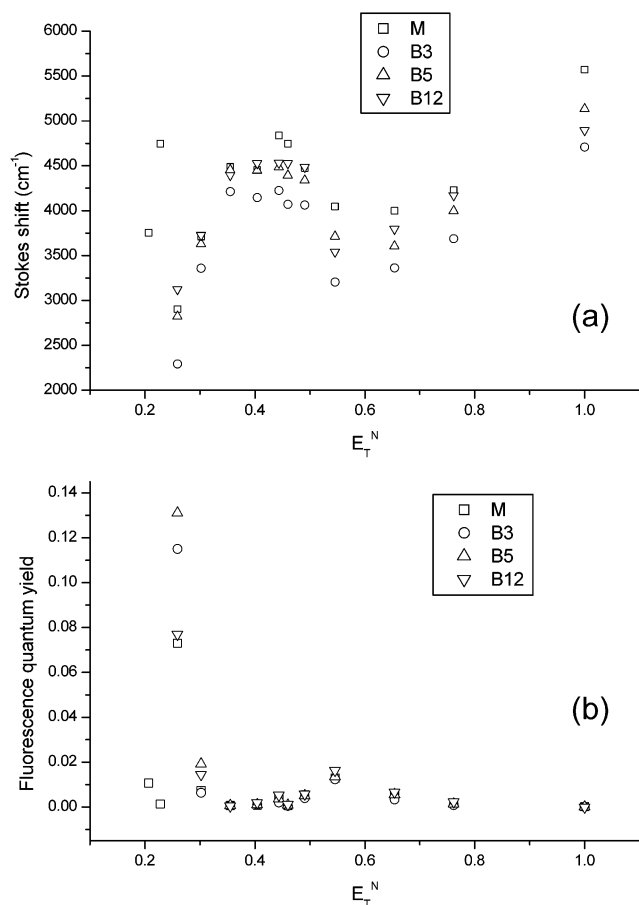


Figure 7. Stokes shift $\Delta\nu$ (a), and the quantum yield (b) versus the empirical polarity scale E_T^N .

regions of E_T^N have different types of intermolecular interaction between the solvent and solute molecules. The most distinct feature of those solvents in region $E_T^N > 0.5$ is that all of these molecules have hydroxyl groups, that is, they are protonic solvents and they can easily form hydrogen bonds with each other and with other molecules. Therefore, the two different regions of E_T^N scale reflect the solute–solvent interaction which not only comes from the polarity of solvent but also from the specific interaction such as hydrogen bonding. Although π^* is applied as the polarizability scale, there are better linearity between the Stokes shifts and polarizability. The biggest difference between π^* and E_T^N is that the former measures not only solvent polarity but also the polarizability, whereas the latter is specific for solvent polarizability.⁴⁶ In both E_T^N and π^* , the scale of polarity of solvents, chloroform is stray, which indicates that the interaction between chloroform and hemicyanine cannot be well expressed by these two parameters.

Figure 7b and 8b show other aspects of the particularity of chloroform among different solvents of hemicyanine solutions. Fluorescence quantum yield of monomer and dimers are measured by steady fluorescence spectra and calculated via the following equation

$$Q_S = Q_R \frac{I_S A_R n_S^2}{I_R A_S n_R^2} \quad (5)$$

where the subscript “S” stands for sample, and “R” for reference; Q is for quantum yield, I for the fluorescence intensity, A for absorbance, and n for optical refractive index. Rhodamine 6G in ethanol, whose fluorescence quantum yield is 95%, is used

as reference. It is shown in Figure 7b and 8b that the fluorescence quantum yield of hemicyanine dyes, both monomer and dimers, in most solvents are very low (less than 3%). However, the chloroform once again reveals its particularity. The fluorescence of these four dyes in chloroform is so intensive that it is visible to naked eyes in the irradiation under normal daylight. This result corresponds with former reports.¹⁸ However, if other polar scales such as Δf and F are used to appraise the solvent effect on fluorescence quantum yield (Figure 5(b) and 6(b)), the result of chloroform is not too difficult to understand. With the scales of Δf and F , chloroform is the weakest polar one among those solvents. It has been confirmed by several reports that a nonradiative TICT state is the most efficient deactive process of excited state of hemicyanine. A higher polar solvent is much more favorable for TICT formation and then the nonradiative transition will take a higher portion of the whole deactive process of excited state. Thus, a nonpolar solvent will benefit the fluorescence transition while a polar solvent will reduce the radiation. Evidently, Δf and F are better scales to describe the relationship between the fluorescence quantum yield and solvent polarity. It is just that the weak polarity of chloroform blocks the formation of high polar TICT state and consequently enhances the fluorescence quantum yield of hemicyanine. If we take both the absorption spectra and the fluorescence spectra into account, chloroform is a really unique solvent for hemicyanine: its effect is similar to a nonpolar solvent in fluorescence emission (high quantum yield), on the other hand, it resembles a polar solvent in absorption (almost no aggregate absorption).

Further observations on the quantum yield data of these solutions reveal another interesting phenomenon. The solutions of 2-propanol have much higher quantum yields ($\sim 1.6\%$) than solutions of methanol ($\sim 0.2\%$) and ethanol ($\sim 0.6\%$) although their polarities are not so different. It is easy to be understood that the formation of TICT state is associated with solvent viscosity. The twisting motion will be inhibited by high viscosity. The viscosity of 2-propanol (2.43 cp) are much higher than that of methanol (0.0547 cp) or ethanol (1.19 cp), the formation of TICT state in 2-propanol is more difficult so that the fluorescence of 2-propanol solution is stronger than in other two alcohol solutions.

In summary, what we have found from these figures is that each parameter has its own limitation, and some are better than others to describe the relationship of solvation and photophysical properties. The figures on the Stokes shift indicate that the specific interaction, such as the hydrogen bonding interaction, cannot be omitted in our system. Although the figures of quantum yields imply that the chloroform is really very unique among all the solvents. Meanwhile, the Stokes shifts of dyes in chloroform are also "strange". At present, we cannot give a better explanation for this uniqueness than we have given in this paper. Although this phenomenon has been reported elsewhere before,^{2,19} no reasonable interpretation has been presented yet. Our attempt to interpret the uniqueness of the chloroform and the relationship between the solvent parameters and the photophysical properties of hemicyanine dyes is only tentative. Further experiments are in process.

3.3. Fluorescence Dynamics of Solution Samples. The experiments of dynamic fluorescence spectra support our assumption on TICT blocking of hemicyanine chloroform solution. In the high polar solvents, such as methanol, the decay of fluorescence is too fast to be determined by our system, whereas in the weak polar solvent chloroform, the decay is prolonged by several tens of times. Figure 9 is a typical plot of

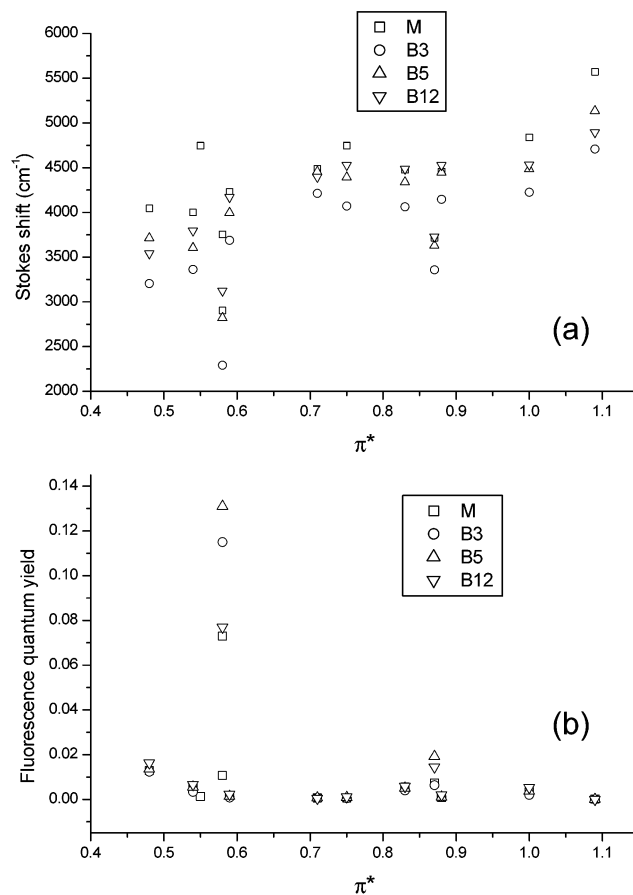


Figure 8. Stokes shift $\Delta\nu$ (a), and the quantum yield (b) versus the empirical polarity scale π^* .

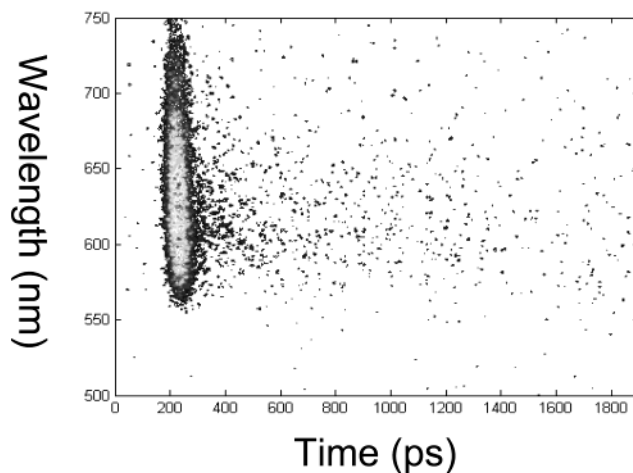


Figure 9. Dynamic fluorescence transients of M in methanol. The contour curves present different fluorescence intensities, these curves reflect the changing tendency of fluorescence intensity and transient spectrum shape with time.

picosecond resolved fluorescence spectra of dyes in methanol. To make it easy, the figure is plotted as contour with decay time and wavelength as the two dimensions. The emission spectra of any transient time and the decay curve of fluorescence at certain wavelengths can be easily imaged from this contour figure. Apparently, in Figure 9 the lifetime of fluorescence is too short to be captured by our streak camera.

Figure 10 shows the results of transient fluorescence spectra of dyes in chloroform. In chloroform, the decay of fluorescence of these dyes are much slower than in methanol, and the decay processes are clearly recorded by streak camera. The most

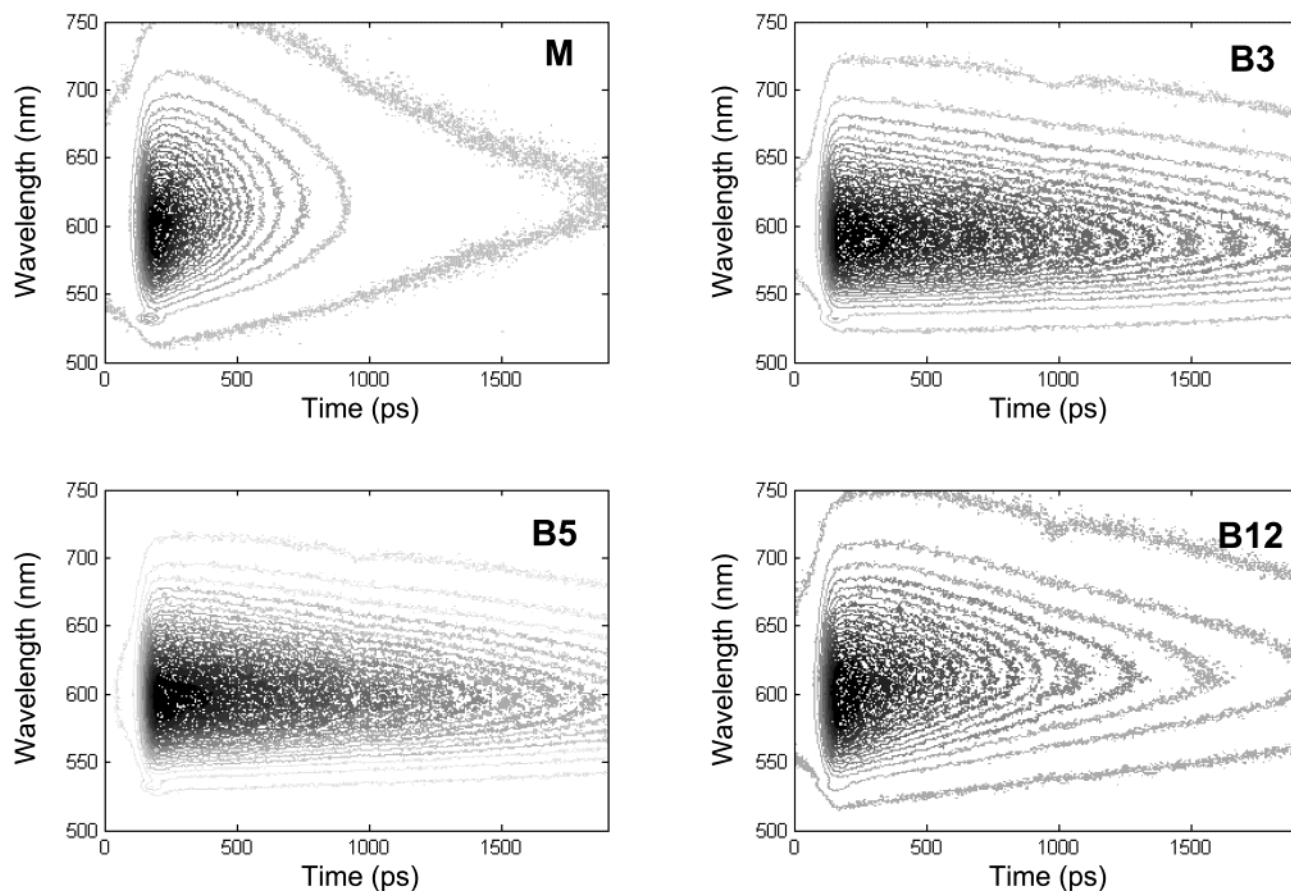
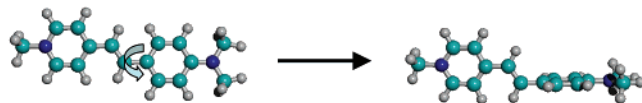


Figure 10. Dynamic fluorescence transient of M, B3, B5, and B12 in chloroform. See text for details.

SCHEME 2: Twisting Motion of Hemicyanine Chromophore through the Torsion of C–C Bond (the aniline ring)



noteworthy characteristic of this figure is that the dimers have more slowly decay than the monomer. This indicates that both the polarity of solvent and the structure of molecule can affect the evolution of excited state of hemicyanine chromophore. It is supposed that the prolonged fluorescence lifetime is possibly due to the hindrance of TICT formation caused by dimerization, that is, the dimerization introduces a large “group” to the hemicyanine chromophore, which makes intramolecular twisting around the C–C bond difficult (Scheme 2). The intensity decay data around the peak position (figures not shown here) of fluorescence spectra can be well fitted by the convolution between a two-component-exponential decay function and the instrumental response curve

$$I(t) = R(t) \otimes [A_1 \exp(-t/\tau_1) + A_2 \exp(-t/\tau_2)] \quad (6)$$

where $I(t)$ is the experimental data at different time t , $R(t)$ the instrumental response function, τ_1 and τ_2 the decay lifetimes of each component, respectively. The result of fitting is demonstrated in Table 2. The results show that both B3 and B5 have longer lifetimes than that of monomer, whereas B12 has a comparable lifetime with that of monomer. In one dimer molecule, when the linkage between the two chromophores is short (3 or 5 methylene groups, which are B3 or B5), the motion

TABLE 2: Fitting Results of the Fluorescence Decay Curves of Dyes in Chloroform by Using Eq 6

sample	A_1 (%)	τ_1 (ps)	A_2 (%)	τ_2 (ps)
M	40.6	84.1	59.4	0.20×10^3
B3	18.8	99.4	81.2	1.20×10^3
B5	33.5	158	66.5	1.31×10^3
B12	68.3	88.7	31.7	0.45×10^3

of one chromophore will strongly correlate to the other one; whereas, in the case of long linkage such as 12 methylene groups, the correlation of motion between the two chromophores are slight. Accordingly, the twisting motion of C–C bond in B12 will be much easier than in B3 or B5. On the basis of the potential energy surfaces of the excited and ground states of hemicyanine (Chart 1), the two components of lifetime fitting results may be attributed to the radiative and nonradiative transitions, respectively.

It is more interesting if the experimental temperature has been decreased to 77 K. The frozen ethanol solutions of these four dyes have similar fluorescence decay lifetime: ~ 2.2 ns. Evidently, this longer value (compared with those values of solutions at room temperature) is mainly due to the twisting block. This result indicates that the twisting of molecule is one of the most important factors to determine the lifetime of the excited state. Hence, when the dyes are dissolved into 2-propanol, which has a higher viscosity, the decay behavior of fluorescence is different from those solvents with lower viscosity (e.g., methanol). The details of the decays in 2-propanol solutions are list as Table 3.

Clearly, the fluorescence emission of 2-propanol solution is red-shifted with decay-time. Thus, the fluorescence decay at the longer wavelength region has a evident rise part (Table 3).

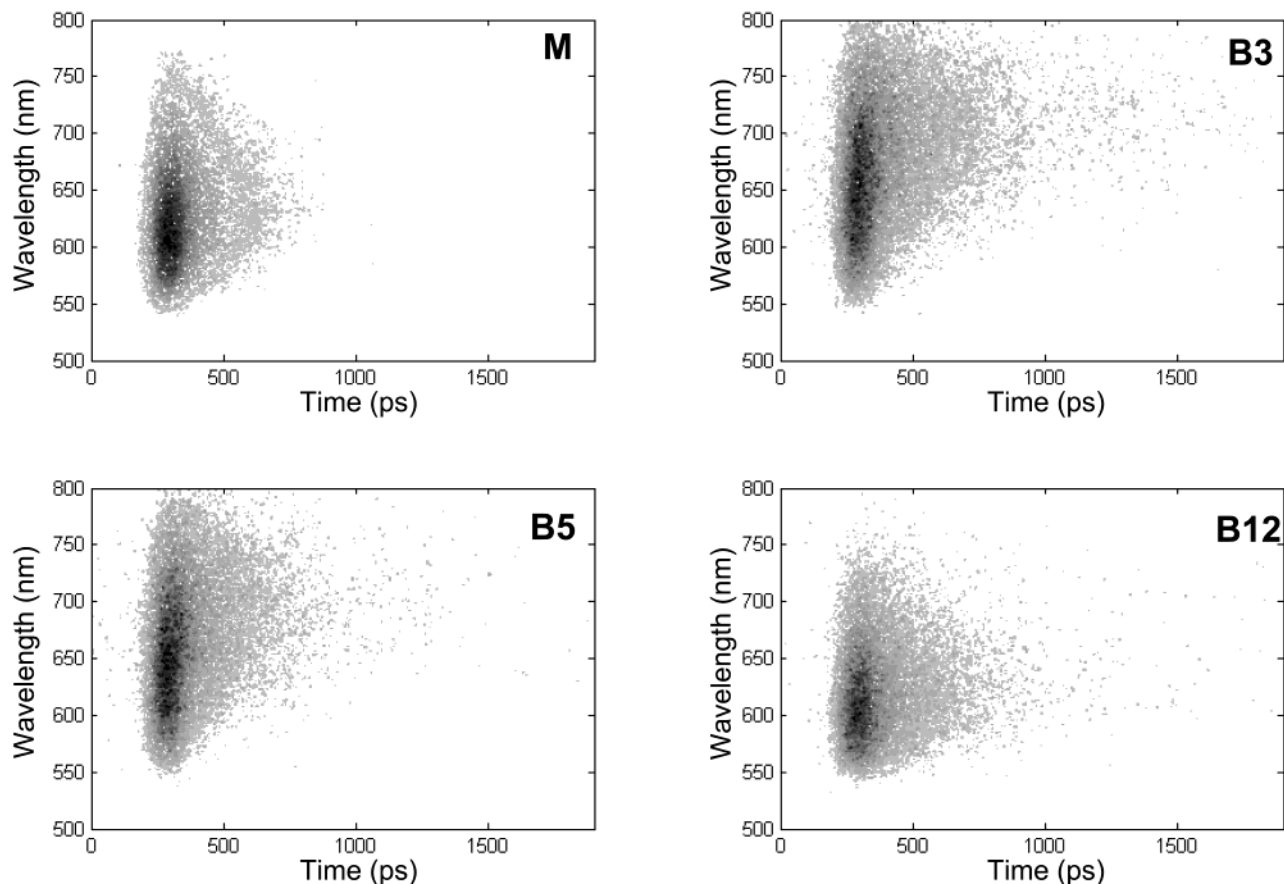


Figure 11. Dynamic fluorescence transient of the LB films (one monolayer) of M, B3, B5, and B12. See text for details.

TABLE 3: Fitting Results of the Fluorescence Decay Curves of Dyes in Ethanol at 77 K

sample	A ₁ (%)	τ ₁ (ps)	A ₂ (%)	τ ₂ (ps)
505~530 nm, 2 decays				
M	72	46	28	417
B3	77	58	23	328
B5	87	59	13	380
B12	91	58	9	380
675~700 nm, rise and decay				
M	-50	66	50	195
B3	-50	46	50	249
B5	-50	57	50	339
B12	-50	58	50	278

This rise component indicates that the high viscosity of 2-propanol can slow the formation of TICT state. This time dependent fluorescence red-shift reflects the energy decreasing of excited state during the TICT formation. Here, the difference of structure is not distinct.

3.4. Fluorescence Dynamics of LB Films. It is natural to suppose that if the hemicyanine chromophores can be confined by some external force to block the twisting of C–C bond, the lifetime will be greatly prolonged and the fluorescence quantum yield will be enhanced simultaneously. It is an easy way to confine the molecules in a two-dimension region to form ordered film by Langmuir–Blodgett technique, by which the density of molecule (area occupied by each molecule) can be well controlled. The details on LB film formation, air–water interface behavior of the derivatives with each long alkyl chain substituted onto each aniline moiety of these four dyes and their applications to the second harmonic generation, as well as photoelectro conversion have been reported elsewhere.⁵⁰ Generally speaking, the dimers have better Langmuir formation ability than monomer, and the limiting areas of hemicyanine chromophore in M,

B3 and B5 are quite similar to each other (0.40–0.45 nm²). This indicates that the dimer has a “folded” conformation and the orientations of hemicyanine chromophores in dimers are similar to that of monomer. Evidently, in these LB films, the hemicyanine chromophores are well confined and nearly parallel. The results of the dynamic fluorescence spectra are shown as contour plots in Figure 11. The decays of B3 and B5 are evidently longer than M and B12, similar to the results in chloroform solutions. More importantly, the lifetimes of these four dyes are much longer than that in methanol solutions, indicating that our supposition is apparently correct: the blocking of TICT formation will prolonged the fluorescence lifetime. However, the fluorescence lifetime of these dyes in LB films are shorter than in ethanol at 77 K, indicating that the twisting of chromophores in LB films are not thoroughly blocked as at low temperature.

The 2-component-decay function fitting of the decay data (Figure 12) of the peak region of these dyes renders the results listed in Table 4. From these values, we see that our supposition does not readily fit into the experimental results. The “lifetime” values of LB films are shorter than those of chloroform solutions when the former should be longer according to our supposition since the chromophores in LB films are surely more confined than in solutions. There might be two main reasons for this mismatch: the polarity of the environment around the hemicyanine chromophore should be taken into consideration and the energy transfer between the chromophores may occur in our system. The relationship between the fluorescence radiation and the polarity of solvent has been thoroughly discussed before, and we would like to consider the polarity of the environment around any hemicyanine chromophore, which is encircled by several closest high-polar molecules/chromophores. This means

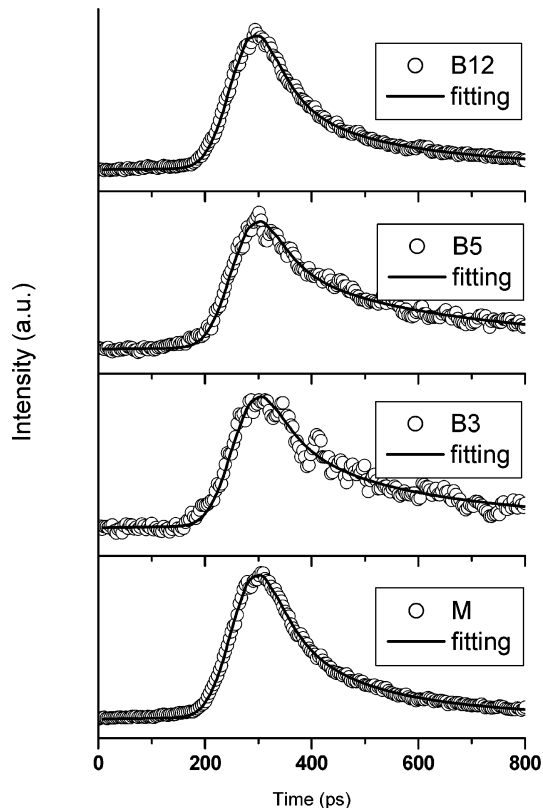


Figure 12. Fluorescence decay data around the peak positions of dyes in LB films. The solid lines are fitting results of eq 7.

TABLE 4: Fitting Results of the Fluorescence Decay Curves of Dyes in LB Films by Using Eq 6

sample	A_1 (%)	τ_1 (ps)	A_2 (%)	τ_2 (ps)
M	76.4	59.6	23.6	268
B3	72.5	74.5	27.5	478
B5	69.7	55.2	30.3	481
B12	80.4	51.9	19.6	321

the hemicyanine in LB film is very much like in high-polar solvent, which will benefit the TICT formation. Therefore, if the chromophore is completely free in LB film, the lifetime will be at the same time scale with in methanol solution. The fact that the lifetime values of these LB films are longer than those of methanol solutions while shorter than those of chloroform solutions confirms that the TICT state formation can be tuned by both polarity of solvent/environment and the steric hindrance of twisting.

It has been mentioned (vide supra) that the area of occupation of each chromophore of M, B3, and B5 are almost the same, indicating that the densities of chromophore in that three LB films are almost the same, and that these LB films have similar microscopic structures as well. Then, suppose the fluorescence is influenced only by TICT formation process, which is tuned only by polarity and steric hindrance, the fluorescence decay behaviors of these three LB films should be also similar to each other. However, the difference between the fluorescence decay of monomer and B3 and B5 are distinct, implying that the dimerization may also affect the deactive processes of the excited state in LB film and there may be some other process involved in the LB films. There are several reports on the energy transfer in LB films within the monolayer or between the different monolayers. In our experiments, the distance between the chromophores is very short (~ 0.4 nm) so that the Förster energy transfer may easily occur within the monolayer. To understand the Förster energy transfer between the chro-

TABLE 5: Fitting Results of the Fluorescence Decay Curves of Dyes in LB Films by Using Eq 7

sample	τ (ps)	A_2/A_1	K	N (molecule/cm ²)
M	3.7×10^2	0.03	3.6	1.0×10^{13}
B3	5.5×10^2	0.07	4.3	1.2×10^{13}
B5	5.3×10^2	0.08	5.3	1.5×10^{13}
B12	3.7×10^2	0.04	4.6	1.2×10^{13}

mophores within the same monolayer, i.e., the 2-dimensional transfer, the following equation can be applied to fit the decay data⁵¹

$$I(t) = R(t) \otimes [A_1 \exp[(-t/\tau) - K(t/\tau)^{1/3}] + A_2 \exp(-t/\tau)] \quad (7)$$

here the first term on the right-hand presents the survival probability of the donor according to the Förster energy transfer process in two-dimensional systems; while the second term expresses the relaxation process of the isolated donor molecules. Their proportion A_2/A_1 is the indicator to the degree of energy transfer.

The fitting results are listed in Table 5. Obviously, if we take Förster energy transfer into consideration, the B3 and B5 are quite different from M and B12. The values of overall decay time (τ) of B3 and B5 are longer than that of M and B12, this is similar to the situation in solution; moreover, the proportions of A_2 to A_1 in B3 and B5 are higher than in M and B12. This means that energy transfer occurs more easily and then the energy loss is more effective in M and B12 monolayer than in B3 or B5.

With K factor, the number density of acceptor (N) can be calculated via eq 8⁵¹

$$N = \frac{3}{4} \frac{K}{\pi R^2} \quad (8)$$

where R is the Förster energy transfer radius (R_0) of chromophore with correction from three-dimension to two-dimension system by a $(3/2)^{1/6}$ factor. The value of R_0 (in Å) can be calculated by

$$R_0 = 0.211 \left[\frac{2}{3} \times n^{-4} \times Q \times \frac{\int_0^\infty F(\lambda) \epsilon_A(\lambda) \lambda^4 d\lambda}{\int_0^\infty F(\lambda) d\lambda} \right]^{1/6} \quad (9)$$

where Q is the fluorescence quantum yield, $F(\lambda)$ the fluorescence intensity in the certain wavelength, and $\epsilon_A(\lambda)$ the absorption coefficient at different wavelength. In our system, these molecules have similar Förster energy transfer ratios around 3 nm. The results (Table 5) of calculation indicate that there is only slight difference of the densities of acceptors of the dye LB films. Meanwhile, the N value of B3 and B5 are even higher than M and B12, illustrating that the decrease of energy transfer proportion does not result from the reduction of acceptor number density. Although the nature of the relationship between the decrease of the energy transfer and the dimerization of the hemicyanine cannot be clearly described at present, this energy transfer decrease may be applied to enhance some other photoactive properties of hemicyanine such as the photoelectro conversion. With the LB films on ITO glass substrates fabricated under similar conditions, B3 and B5 have distinctly higher (0.6% and 0.5%, respectively) photoelectro conversion quantum yields than M and B12 (both 0.3%). This enhancement with dimerization puzzled us for a long time, until we investigated the energy transfer between chromophores within monolayer. From

the perspective of photoelectron ejection between the dye's excited state and the semiconductor, the longer the lifetime of dye's excited state, the higher the possibility for electron transfer to generate the photocurrent becomes. Decreasing the energy transfer within the monolayer will certainly reduce the energy loss via migration and consequently benefit the photocurrent generation. More experiments are being carried out to explore the details of the relationship between the dimerization and the photophysical properties of hemicyanine.

4. Summary

A series of hemicyanine dimers has been synthesized and the steady state absorption and fluorescence spectra, solvent effects on spectra, and dynamic fluorescence spectra in different solvents and in LB films have been investigated. In those weak-polar solvents, all of the dyes are difficult to dissolve and H-aggregate is formed. Negative solvatochromic behavior is found in each dye and several polarity/polarizability scales have been used to describe the shifts of spectra with the change of solvents. Although the tendency is clear, the interaction between hemicyanine chromophore and solvent molecules are too complex to be perfectly interpreted by any one of these parameters. In a high-polar solvent, all of the dyes have extremely low fluorescence quantum yields, whereas in a weak-polar solvent such as chloroform, the fluorescence quantum yield greatly increases. The fluorescence decay of these dyes in methanol is too rapid to be observed by streak camera, whereas the decay in chloroform solution is much slower and can be well recorded. The analysis of decay lifetime indicates that the fluorescence can be enhanced via blocking the twisting of chromophore, which forms a nonradiative TICT state. Furthermore, the TICT formation can be tuned by both environmental polarity and steric hindrance. The decay lifetime analysis of the LB films of these dyes implies that there might be energy transfer within the monolayer. The decreased energy transfer proportions of the LB films of B3 and B5 well explain their enhanced photoelectro conversion quantum yields.

Acknowledgment. This work is supported by the State Key Program of Fundamental Research (G1998061308 and 2001CCD04300), the National Natural Science Foundation of China (20023005, and 59872001) and the Doctoral Program of Higher Education (99000132). Prof. Yuxiang Weng and Prof. Hongfei Wang are also gratefully acknowledged by Y. H. for their kind help.

References and Notes

- (1) For example, see Jones, M. A.; Bohn, P. W. *Anal. Chem.* **2000**, *72*, 3776.
- (2) Ehardt, H.; Fromherz, P. *J. Phys. Chem.* **1989**, *93*, 7717.
- (3) Zhao, C. F.; Gvishi, R.; Narang, U.; Ruland, G.; Prasad, P. N. *J. Phys. Chem.* **1996**, *100*, 4526.
- (4) Abraham, U. *An Introduction to Ultrathin Organic Films: From Langmuir-Blodgett to Self-Assembly*; Academic Press: Boston, 1991.
- (5) He, G. S.; Bhawalkar, J. D.; Zhao, C. F.; Prasad, P. N. *Appl. Phys. Lett.* **1995**, *67*, 2433.
- (6) Chemla, D. S.; Zyss, J. *Nonlinear Optical Properties of Organic Molecules and Crystals*; Academic Press: Orlando, 1987.
- (7) Ashwell, G. J.; Jackson, P. D.; Crossland, W. A. *Nature* **1994**, *368*, 438.
- (8) Duan, X. M.; Konami, H.; Okada, S.; Oikawa, H.; Matsuda, H.; Nakanishi, H. *J. Phys. Chem.* **1996**, *100*, 17 780.
- (9) Ashwell, G. J.; Jackson, P. D.; Lochun, D.; Thompson, P. A.; Crossland, W. A.; Bahra, G. S.; Brown, C. R.; Jasper, C. *Proc. R. Soc. London A* **1994**, *445*, 385.
- (10) Xu, J.; Lu, X.; Zhou, G.; Zhang, Z. *Thin Solid Films*, **1998**, *312*, 295.
- (11) Kim, O.-K.; Choi, L.-S.; Zhang, H.-Y.; He, X.-H.; Shih, Y.-H. *J. Am. Chem. Soc.* **1996**, *118*, 12 220.
- (12) Wu, D. G.; Huang, C. H.; Gan, L. B.; Zhang, W.; Zheng, J.; Luo, H. X.; Li, N. Q. *J. Phys. Chem. B* **1999**, *103*, 4377.
- (13) Wu, D. G.; Huang, C. H.; Huang, Y.; Gan, L. B.; Yu, A. C.; Ying, L. M.; Zhao, X. S. *J. Phys. Chem. B* **1999**, *103*, 7130.
- (14) Lang, A. D.; Zhai, J.; Huang, C. H.; Gan, L. B.; Zhao, Y. L.; Zhou, D. J.; Chen, Z. D. *J. Phys. Chem. B* **1998**, *102*, 1424.
- (15) Wang, Z. S.; Li, F. Y.; Huang, C. H.; Wang, L.; Wei, M.; Jin, L. P.; Li, N. Q. *J. Phys. Chem. B* **2000**, *104*, 9676.
- (16) Joshi, M. P.; Deleon, R. L.; Prasad, P. N.; Garvey, J. F. *J. Appl. Phys.* **1999**, *85*, 3928.
- (17) Cheng, P. C.; Pan, S. J.; Shih, A.; Kim, K.-S.; Liou, W. S.; Park, M. S. *J. Microscopy* **1998**, *189*, 199.
- (18) Ehardt, H.; Fromherz, P. *J. Phys. Chem.* **1989**, *93*, 7717.
- (19) (a) Song, Q.; Bohn, P. W.; Blanchard, G. J. *J. Phys. Chem. B* **1997**, *101*, 8863. (b) Evans, C. E.; Song, Q.; Bohn, P. W. *J. Phys. Chem.* **1993**, *97*, 12302. (c) Evans, C. E.; Bohn, P. W. *J. Am. Chem. Soc.* **1993**, *115*, 3106. (d) Habashy, M. M.; El-Sawawi, F.; Antonious, M. S.; Sheriff, A. K.; Abdel-Mottaleb, M. S. A. *Ind. J. Chem. A* **1985**, *24*, 908.
- (20) Kim, J.; Lee, M. *J. Phys. Chem. A* **1999**, *103*, 3378. and references therein.
- (21) Herbich, J.; Grabowski, Z. R.; Wojtowicz, H.; Golankiewicz, K. *J. Phys. Chem.* **1989**, *93*, 3439.
- (22) Grabowski, Z. R. *Pure Appl. Chem.* **1992**, *64*, 1249.
- (23) Maus, M.; Rettig, W.; Bonafoux, D.; Lapouyade, R. *J. Phys. Chem.* **1999**, *103*, 3388.
- (24) Bhattacharyya, K.; Chowdhury M. *Chem. Rev.* **1993**, *93*, 507.
- (25) Rettig, W. *Top. Curr. Chem.* **1994**, *169*, 253.
- (26) Cao, X.; Tolbert, R. W.; McHale, J. L.; Edwards, W. D. *J. Phys. Chem. A* **1998**, *102*, 2739.
- (27) Cao, X.; McHale, J. L. *J. Chem. Phys.* **1998**, *109*, 1901.
- (28) McHale, J. L. *Acc. Chem. Res.* **2001**, *34*, 265.
- (29) For example, see Wurthner, F.; Yao, S. *Angew. Chem., Int. Ed.* **2000**, *39*, 1978.
- (30) Bazan, G. C.; Oldham, W. J.; Lachicotte, R. J.; Tretiak, S.; Chernyak, V.; Mukamel, S. *J. Am. Chem. Soc.* **1998**, *120*, 9188.
- (31) Song, X.; Perlstein, J.; Whitten, D. G. *J. Phys. Chem. A* **1998**, *102*, 5440.
- (32) Mishra, J. K.; Behera, P. K.; Parida, S. K.; Mishra, B. K. *Ind. J. Chem.* **1992**, *31B*, 118.
- (33) Mishra, B. K.; Kuanar, M.; Mishra, A.; Behera, G. B. *Bull. Chem. Soc. Jpn.* **1996**, *69*, 2581.
- (34) Chibisov, A. K.; Zakharova, G. V.; Gerner, H.; Sogulyaev, Y. A.; Mushkalo, I. L.; Tolmachev, A. I. *J. Phys. Chem.* **1995**, *99*, 886.
- (35) Zeena, S.; Thomas, K. G. *J. Am. Chem. Soc.* **2001**, *123*, 7859.
- (36) Bartholomew, G. P.; Bazan, G. C. *Acc. Chem. Res.* **2001**, *34*, 30.
- (37) Lu, L.; Lachicotte, R. J.; Penner, T. L.; Peristein, J.; Whitter, D. G. *J. Am. Chem. Soc.* **1999**, *121*, 8146.
- (38) Mcree, E. G.; Kasha, M. *J. Chem. Phys.* **1958**, *28*, 721.
- (39) Lakowicz, J. R. *Principles of Fluorescence Spectroscopy*, 2nd ed.; Kluwer Academic/Plenum Publishers: New York, 1999.
- (40) Reichardt, C. *Solvents and Solvent Effects in Organic Chemistry*, 2nd ed.; VCH: Weinheim, 1998.
- (41) Narang, U.; Zhao, C. F.; Bhawalkar, J. D.; Bright, F. V.; Prasad, P. N. *J. Phys. Chem.* **1996**, *100*, 4521.
- (42) Baur, J. W.; Alexander, M. D., Jr.; Banach, M.; Denny, L. R.; Reinhardt, B. A.; Vaia, R. A. *Chem. Mater.* **1999**, *11*, 2899.
- (43) Horng, M. L.; Gardecki, J. A.; Papazyan, A.; Maroncelli, M. *J. Phys. Chem.* **1995**, *99*, 17 311.
- (44) Gulbinas, V.; Kodis, G.; Jursenas, S.; Valkunas, L.; Gruodis, A.; Mialocq, J.-C.; Pommeret, S.; Gustavsson, T. *J. Phys. Chem. A* **1999**, *103*, 3969.
- (45) Abe, T.; Kawai, A.; Kajii, Y.; Shibuya, K.; Obi, K. *J. Phys. Chem. A* **1999**, *103*, 1457.
- (46) Reynolds, L.; Gardecki, J. A.; Frankland, S. J. V.; Horng, M. L.; Maroncelli, M. *J. Phys. Chem.* **1996**, *100*, 10 337.
- (47) Kamlet, M. J.; Abboud, J. L.; Taft, R. W. *J. Am. Chem. Soc.* **1977**, *99*, 6027.
- (48) Brooker, L. G. S.; Craig, A. C.; Heseltine, D. W.; Jenkins, P. W.; Lincoln, L. L. *J. Am. Chem. Soc.* **1965**, *87*, 2443.
- (49) Habashy, M. M.; El-Zawawi, F.; Antonious, M. S.; Sheriff, A. K.; Abdel-Mottaleb, M. S. A. *Ind. J. Chem.* **1985**, *24A*, 908.
- (50) Huang, Y.; Cheng, T.; Li, F.; Huang, C.; Hou, T.; Yu, A.; Zhao, X.; Xu, X. *J. Phys. Chem. B* **2002**, *106*, 10020.
- (51) Akimoto, S.; Ohmori, A.; Yamazaki, I. *J. Phys. Chem. B* **1997**, *101*, 3753. and references therein.